

Theoretical Studies of the Gas-Phase Identity Nucleophilic Substitution Reactions of Cyclopentadienyl Halides

Ikchoon Lee,* Hong Guang Li, Chang Kon Kim,
Bon-Su Lee, Chan Kyung Kim, and Hai Whang Lee

Department of Chemistry Inha University Incheon 402-751, Korea

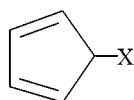
Received February 21, 2003

The gas phase identity nucleophilic substitution reactions of halide anions ($X = F, Cl, Br$) with cyclopentadienyl halides (**1**) are investigated at the B3LYP/6-311+G**, MP2/6-311+G** and G2(+)MP2 levels involving five reaction pathways: σ -attack S_N2 , β - S_N2' -syn, β - S_N2' -anti, γ - S_N2' -syn and γ - S_N2' -anti paths. In addition, the halide exchange reactions at the saturated analogue, cyclopentyl halides (**2**), and the monohapto circumambulatory halide rearrangements in **1** are also studied at the same three levels of theory. In the σ -attack S_N2 transition state for **1** weak positive charge develops in the ring with $X = F$ while negative charge develops with $X = Cl$ and Br leading to a higher energy barrier with $X = F$ but to lower energy barriers with $X = Cl$ and Br than for the corresponding reactions of **2**. The π -attack β - S_N2' transition states are stabilized by the strong $n_C-\pi^*_{C=C}$ charge transfer interactions, whereas the π -attack γ - S_N2' transition states are stabilized by the strong $n_C-\sigma^*_{C-X}$ interactions. For all types of reaction paths, the energy barriers are lower with $X = F$ than Cl and Br due to the greater bond energy gain in the partial C-X bond formation with $X = F$. The β - S_N2' paths are favored over the γ - S_N2' paths only with $X = F$ and the reverse holds with $X = Cl$ and Br . The σ -attack S_N2 reaction provides the lowest energy barrier with $X = Cl$ and Br , but that with $X = F$ is the highest energy barrier path. Activation energies for the circumambulatory rearrangement processes are much higher (by more than 18 kcal mol⁻¹) than those for the corresponding S_N2 reaction path. Overall the gas-phase halide exchanges are predicted to proceed by the σ -attack S_N2 path with $X = Cl$ and Br but by the β - S_N2' -anti path with $X = F$. The barriers to the gas-phase halide exchanges increase in the order $X = F < Br < Cl$, which is the same as that found for the gas-phase identity methyl transfer reactions.

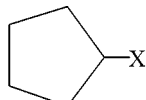
Key Words : Gas-phase, Nucleophilic substitution, Cyclopentadienyl halides, G2(+)MP2

Introduction

The experimental studies of the nucleophilic substitution reactions of cyclopentadienyl halides ((CH)₅X; **1**) by Breslow *et al.*¹ with $X = Br$ and I have indicated that cyclopentadi-

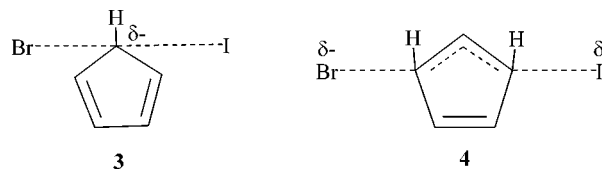


1



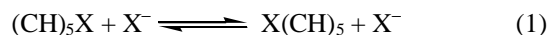
2

enyl iodide (**1** with $X = I$) reacts with Br^- ($Bu_4N^+Br^-$) to give cyclopentadienyl bromide (**1** with $X = Br$) *ca.* 10 times as rapidly as cyclopentyl iodide (**2** with $X = I$) reacts in 1/1 (v/v) CCl_4-CH_3CN at 25.0 °C. The reactivity of cyclopentadienyl bromide (**1** with $X = Br$) with I^- ($Bu_4N^+I^-$) was found to be even greater, *ca.* 10² times than that of cyclopentyl bromide (**2** with $X = Br$). They invoked (aromatic) cyclopentadienyl anionic character on the carbon atom in S_N2 reactions, **3**, and another possibility of a γ - S_N2' reaction, **4**, to explain the higher reactivity of **1** than **2**. However they were not able to provide satisfactory mechanistic infor-



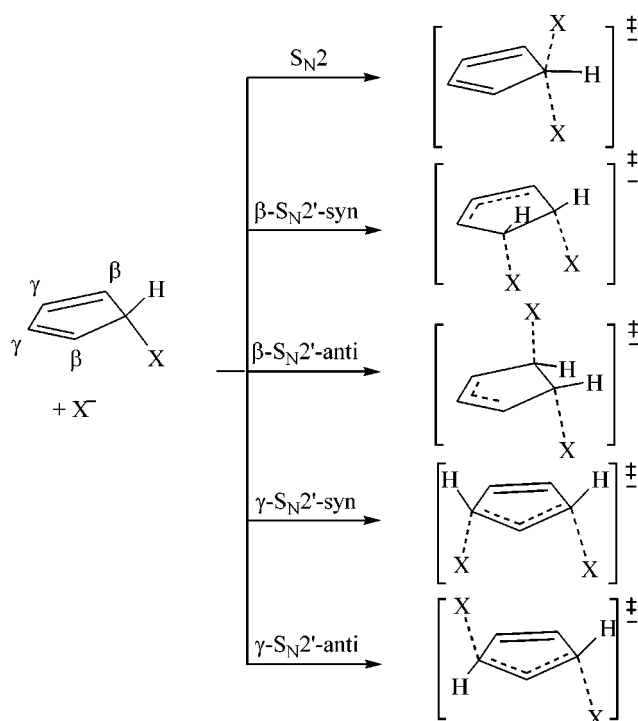
mation for the facts that (i) the reaction of bromide (**1** with $X = Br$) with I^- is *ca.* 10² times more accelerated than is the reaction of iodide (**1** with $X = I$) with Br^- under the same reaction condition, and (ii) the cyclopentadienyl halides (**1**) are completely unreactive under S_N1 solvolytic conditions, but with added halide salts ($Bu_4N^+X^-$) they are significantly more reactive than are the cyclopentyl halides (**2**).

In order to present plausible answers to these problems by elucidating the detailed mechanism involved in the reactions of halide anions with cyclopentadienyl halides, we have undertaken a high level ab initio molecular orbital study on the gas-phase identity nucleophilic substitution reactions of **1**, eq. 1 with $X = F, Cl$ and Br . The nucleophilic substitution reaction of **1** presents a variety of reaction pathways that



may involve a ring structure in the transition state (TS) with aromatic (anionic) or antiaromatic (cationic) character.² We have considered altogether 5 types of possible reaction paths

*Corresponding Author. Fax: +82-32-865-4855; E-mail: ilee@inha.ac.kr



Scheme 1. Various reaction pathways.

shown in Scheme 1. In addition, we have extended the studies (i) to the corresponding S_N2 reactions of the saturated analogues (*s*- S_N2), cyclopentyl halides, **2**, and (ii) to the sigmatropic 1,5-shifts of halide (circumambulatory rearrangement)³ within the cyclopentadienyl ring.

Computational Methods

Calculations were performed at the B3LYP/6-311+G^{**}, MP2/6-311+G^{**} and G2(+)MP2 levels using the Gaussian 98 programs.⁴ In the G2(+)MP2 level, diffuse functions were added to the standard G2MP2 method in order to get more accurate geometries and thermochemical data. Stationary points were characterized with analytical second derivatives. Enthalpies (ΔH^\ddagger) and free energies (ΔG^\ddagger) of activation at 298 K were calculated using vibrational contributions calculated with the use of harmonic frequencies computed at the B3LYP/6-311+G^{**} and MP2/6-311+G^{**} levels and scaled by the appropriate factors.⁵ Activation parameters are reported relative to the separated reactants level. The natural bond orbital (NBO) analyses⁶ were carried out to determine the proximate bond-antibond (which includes $n-\sigma^*$, $n-\pi^*$, $\sigma-p^*$, $\sigma-\sigma^*$, etc) charge-transfer delocalization energies, $\Delta E_{\sigma-\sigma^*}^{(2)}$ in eq. 2, in the substrates and transition states (TSs),

$$\Delta E_{\sigma-\sigma^*}^{(2)} = -\sum \frac{2F^2 \sigma\sigma^*}{\epsilon_{\sigma^*} - \epsilon_{\sigma}} \quad (2)$$

and natural population analyses (NPA)⁶ were carried out. The percentage bond order changes upon TS formation, $\% \Delta n^\ddagger$,⁷ were determined using eq. 3, where r^\ddagger , r_R and r_P are the bond lengths in the TS, reactant and product respectively and

$$\% \Delta n^\ddagger = \frac{[\exp(-r^\ddagger/a) - \exp(-r_R/a)]}{[\exp(-r_P/a) - \exp(-r_R/a)]} \times 100 \quad (3)$$

a was set to 0.6 for bond orders less than one and to 0.3 for bond orders greater than one.

Results and Discussion

Reactants and Reactant Complexes (RCs). The reactant structures are presented in Figures 1-3. In general, bond lengths in the ring are slightly longer with X = F than with Cl and Br. The C-X bond in all cases is shorter than that in the saturated analogue, cyclopentyl halides (**2**), e.g., for X = F, d_{C-F} = 1.392 Å for **1** and 1.409 Å for **2**. A stable adduct is formed only in the β - S_N2' -anti reaction path with X = F in a triple-well potential energy surface. In all other cases, double-well potential energy profiles are obtained, in which there are two identical ion-dipole complexes (RCs) on either side of the central reaction barrier. The structures of the reactant complexes (RCs) are shown in **S1** (Supporting Information). For the γ - S_N2' paths with X = Cl and Br, the RCs have bifurcated structures with X loosely bonded to two hydrogens on the γ,γ -carbons at the B3LYP/6-311+G^{**} level. We failed to locate the RC at the MP2 level for the S_N2 path with X = F and that shown in **S1** is obtained at the RHF/6-311+G^{**} result. The complexation energies (ΔE_{RC}) or well-depths range from -6 to -18 kcal mol⁻¹ as shown in **S1**.

The σ -attack S_N2 reactions. The halide anion attacks at

Table 1. Activation Parameters^a for the Identity Halide Exchange Reactions of Cyclopentadienyl Halide, at the B3LYP/6-311+G^{**} Level (in kcal mol⁻¹)

X	Paths	ΔE^\ddagger	ΔE_{ZPE}^\ddagger	ΔH^\ddagger ^b	$-T\Delta S^\ddagger$ ^b	ΔG^\ddagger ^b
F	S_N2	0.46	-0.40	-0.76	8.14	7.38
	(<i>s</i> - S_N2) ^c	(-2.06)	(-2.58)	(-3.21)	(9.17)	(5.97)
	β - S_N2' -syn	-3.30	-3.84	-4.70	8.88	4.18
	β - S_N2' -anti TS	-9.59	-10.10	-10.79	8.28	-2.51
	Int ^d	-11.26	-11.55	-12.00	8.31	-3.68
	γ - S_N2' -syn	-4.02	-4.78	-5.43	8.23	2.80
Cl	S_N2	2.11	1.45	1.27	7.53	8.79
	(<i>s</i> - S_N2) ^c	(2.54)	(1.78)	(1.43)	(8.44)	(9.87)
	β - S_N2' -syn	27.69	26.41	26.07	7.33	33.41
	β - S_N2' -anti	7.84	6.91	6.76	7.25	14.01
	γ - S_N2' -syn	6.86	6.31	6.00	7.21	13.20
	γ - S_N2' -anti	5.50	4.91	4.69	7.36	12.05
Br	S_N2	-0.09	-0.68	-0.83	7.46	6.63
	(<i>s</i> - S_N2) ^c	(1.78)	(0.90)	(0.69)	(7.66)	(8.34)
	β - S_N2' -syn	27.28	26.06	25.95	6.44	32.39
	β - S_N2' -anti	4.37	3.44	3.54	7.07	10.40
	γ - S_N2' -syn	4.59	4.13	3.82	7.13	10.95
	γ - S_N2' -anti	3.09	2.56	2.38	7.24	9.61

^aCorrected for zero-point vibrational energy with the scaling factor of 0.9806. ^bAt 298 K. ^cFor the saturated reactants (i.e., for cyclopentyl halides). ^dFor intermediate.

Table 2. Activation Parameters^a for the Identity Halide Exchange Reactions of Cyclopentadienyl Halide, at the MP2/6-311+G** Level (in kcal mol⁻¹)

X	Paths	ΔE^\ddagger	$\Delta E^\ddagger_{\text{ZPE}}$	ΔH^\ddagger^b	$-\text{T}\Delta S^\ddagger^b$	ΔG^\ddagger^b
F	S _N 2	6.99	6.19	5.73	8.44	14.17
	(s-S _N 2) ^c	(3.91)	(3.56)	(2.82)	(9.33)	(12.15)
	β-S _N 2'-syn	-1.88	-1.92	-2.81	8.89	6.08
	β-S _N 2'(A) TS	-5.96	-6.12	-6.84	8.36	1.51
	Int ^d	-9.78	-9.71	-10.16	8.19	-1.97
	γ-S _N 2'-syn	-1.73	-2.04	-2.80	8.41	5.62
γ-S _N 2'-anti	0.40	-0.05	-0.69	8.68	7.96	
Cl	S _N 2	8.79	7.71	7.54	7.80	15.34
	(s-S _N 2) ^c	(10.33)	(9.66)	(9.29)	(8.18)	(17.47)
	β-S _N 2'-syn ^e	24.28	23.37	22.31	9.43	31.75
	β-S _N 2'-anti	11.04	10.49	10.04	8.38	18.42
	γ-S _N 2'-syn	11.94	11.81	11.32	7.79	19.11
	γ-S _N 2'-anti	13.35	13.13	12.76	7.96	20.72
Br	S _N 2	5.18	4.29	4.10	8.03	12.13
	(s-S _N 2) ^c	(8.86)	(8.39)	(8.02)	(8.28)	(16.30)
	β-S _N 2'-syn ^e	30.64	29.58	28.63	9.40	38.03
	β-S _N 2'-anti	10.76	10.52	10.10	8.45	18.55
	γ-S _N 2'-syn	10.24	10.25	9.74	8.07	17.81
	γ-S _N 2'-anti	11.35	11.19	10.84	8.07	18.91

^aThermal data were taken from the MP2/6-31+G* level and zero-point vibrational energies were corrected with the scaling factor of 0.9670. ^bAt 298 K. ^cFor the saturated reactants, *i.e.*, cyclopentyl halides. ^dFor intermediate. ^eTwo imaginary frequencies (second-order saddle point).

Table 3. Activation Parameters^a for the Identity Halide Exchange Reactions of Cyclopentadienyl Halide, at the G2(+)/MP2//MP2/6-311+G** Level (in kcal mol⁻¹)

X	Paths	ΔE^\ddagger	$\Delta E^\ddagger_{\text{ZPE}}$	ΔH^\ddagger^b	$-\text{T}\Delta S^\ddagger^b$	ΔG^\ddagger^b
F	S _N 2	1.32	0.52	0.05	8.44	8.49
	(s-S _N 2) ^c	(-1.25)	(-1.60)	(-2.34)	(9.33)	(6.99)
	β-S _N 2'-syn	-5.08	-5.13	-6.01	8.89	2.88
	β-S _N 2'-anti TS	-8.48	-8.65	-9.37	8.36	-1.02
	Int ^d	-12.34	-12.27	-12.72	8.19	-4.53
	γ-S _N 2'-syn	-4.17	-4.48	-5.24	8.41	3.19
γ-S _N 2'-anti	-2.25	-2.68	-3.32	8.68	5.33	
Cl	S _N 2	3.55	2.47	2.30	7.80	10.10
	(s-S _N 2) ^c	(4.52)	(3.84)	(3.47)	(8.18)	(11.66)
	β-S _N 2'-syn ^e	26.14	25.23	24.17	9.43	33.60
	β-S _N 2'-anti	12.81	12.25	11.80	8.38	20.19
	γ-S _N 2'-syn	11.53	11.41	10.92	7.79	18.71
	γ-S _N 2'-anti	11.68	11.46	11.09	7.96	19.05
Br	S _N 2	1.99	1.09	0.91	8.03	8.94
	(s-S _N 2) ^c	(4.26)	(3.79)	(3.42)	(8.28)	(11.70)
	β-S _N 2'-syn ^e	31.23	30.18	29.23	9.40	38.62
	β-S _N 2'-anti	10.82	10.59	10.17	8.45	18.62
	γ-S _N 2'-syn	9.80	9.81	9.31	8.07	17.38
	γ-S _N 2'-anti	9.70	9.54	9.18	8.07	17.25

^aThermal data were taken from the MP2/6-31+G* level and zero-point vibrational energies were corrected with the scaling factor of 0.9670. ^bAt 298 K. ^cFor the saturated reactants, *i.e.*, cyclopentyl halides. ^dFor intermediate. ^eTwo imaginary frequencies (second-order saddle point).

the C₁ atom and a trigonal bipyramidal pentacoordinate (TBP-5C) TS (**3**) is formed in which the cyclopentadienyl ring provides two equatorial ligands. The reactions proceed through typical double-well potential energy surfaces. As have been pointed out by Breslow *et al.*¹ this TS will be extremely unstable, if positive charge develops in the TS within the ring, due to the antiaromatic character of the cyclopentadienyl cation. By contraries, if negative charge develops in the ring, the TS will be stabilized due to the aromatic character of the cyclopentadienyl anion. The energetics summarized in Tables 1-3 reveals that the activation energies (ΔE^\ddagger and ΔG^\ddagger) for the σ -attack S_N2 reaction of fluoride anion with cyclopentadienyl fluoride (**1** with X = F) are higher by $\delta\Delta G^\ddagger = \Delta G^\ddagger(\text{S}_{\text{N}2}) - \Delta G^\ddagger(\text{s-S}_{\text{N}2}) = +1.5$ kcal mol⁻¹ at the G2(+) MP2 level than that with cyclopentyl fluoride (s-S_N2; **2** with X = F), while those for the reactions of **1** with X = Cl and Br are lower by $\delta\Delta G^\ddagger = -1.6$ and -2.8 kcal mol⁻¹ respectively than those for the corresponding reactions of **2** with Cl and Br at the G2(+)/MP2 level. This should indicate that there is an unfavorable electronic effect within the unsaturated ring in the reaction of **1** with X = F, in contrast there is a favorable effect within the ring in the reactions of **1** with Cl and Br, compared with the reactions of **2** with the respective halide. The percentage bond order changes upon TS formation, % $\Delta n^{\ddagger 7}$ (**S2**), and the NPA charge⁶ analyses (**S3**) show that the degrees of bond making and cleavage are approximately 50% in all cases with the NPA charges at the C₁ atom in the TS of $q_1^\ddagger = +0.149$ (X = F), -0.112 (Cl) and -0.159 (Br). These results clearly

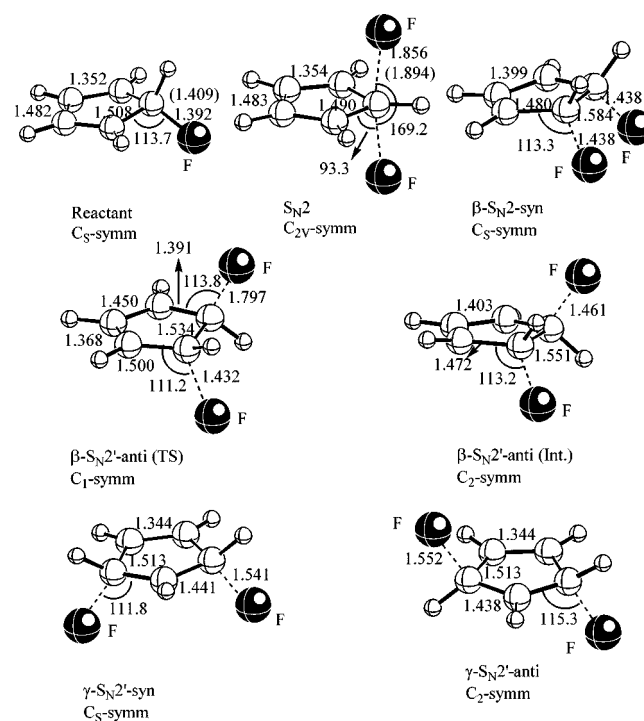


Figure 1. Structures of reactant and transition states for the identity fluoride exchange reactions of cyclopentadienyl fluoride, calculated at the MP2/6-311+G** level (bond lengths in Å, and angles in degrees). Values in parentheses are for cyclopentyl fluoride.

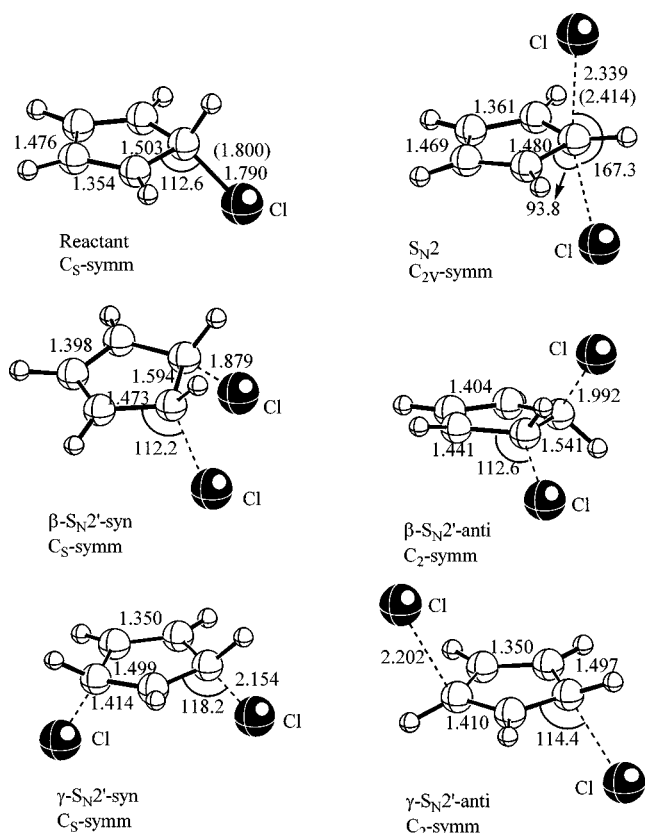
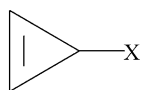


Figure 2. Structures of reactant and transition states for the identity chloride exchange reactions of cyclopentadienyl chloride, calculated at the MP2/6-311+G* level (bond lengths in Å, and angles in degrees). Values in parentheses are for cyclopentyl chloride.

show that the reaction of fluoride (**1** with X = F) is unfavorable whereas those of chloride and bromide (**1** with X = Cl and Br) are favorable over the corresponding reactions with **2** due to antiaromatic cationic charge (for X = F) and aromatic anionic charge (for X = Cl and Br) development in the TSs, respectively.

The TS structures are shown in Figures 1-3. The C-F bonds in the distorted TBP-5C TS with C_{2V} symmetry for **1** with X = F are longer by 0.038 Å than the corresponding values in the TS for **2** with X = F. In contrast, however, they are much shorter than the corresponding values ($d_{C-F}^{\ddagger} = 2.069$ Å) in the σ -attack S_N2 TS for cyclopropenyl fluoride (**5**, X = F), by 0.213 Å.⁸ In the latter, the TS has an “open” structure in a dissociative type S_N2 process so that the cyclopropenium ring has strong delocalized cationic (aromatic) character. In fact all the C-X bonds in the σ -attack S_N2 TSs for the identity exchange of cyclopentadienyl halides (Figures 1-3) are much shorter (by 0.342 Å for X = Cl and 0.395 Å for X = Br at the MP2 level) than the corresponding values for cyclopropenyl halides, **5** ((CH)₃X).⁸



5

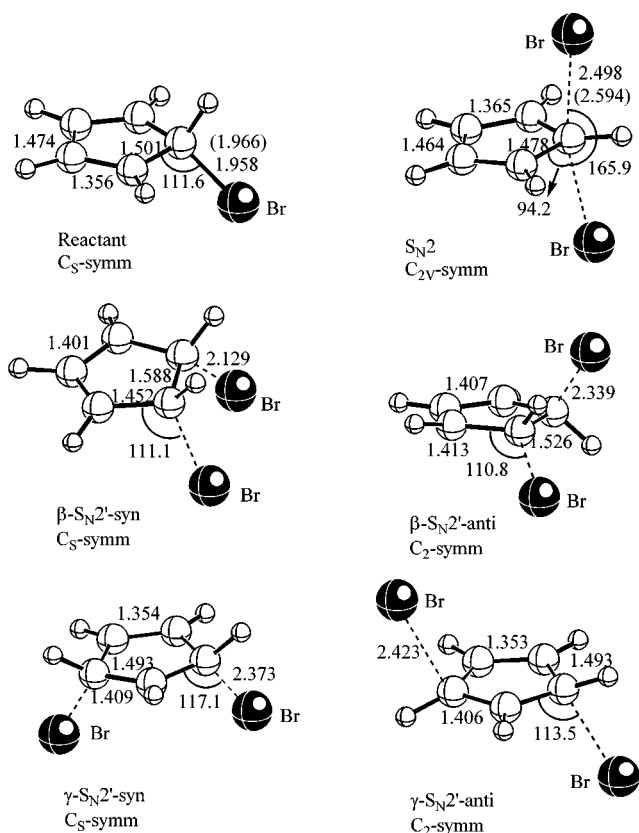


Figure 3. Structures of reactant and transition states for the identity bromide exchange reactions of cyclopentadienyl bromide, calculated at the MP2/6-311+G* level (bond lengths in Å, and angles in degrees). Values in parentheses are for cyclopentyl bromide.

These trends of forming tighter TSs (**S2**) in the S_N2 reactions with **1** than with cyclopropenyl halides (**5**) are of course to preserve as much as possible the (aromatic) anionic ring character in the TSs for the associative type S_N2 reactions of **1**, in contrast to the preferred (aromatic) cationic ring character in the TSs for the dissociative type S_N2 reactions of **5**.

In the TBP-5C TS (Figure 1) an empty p orbital develops as the leaving group, F^- , departs, and leads to strong electronic charge delocalization from the lone pair orbitals (one p and two sp^3 types) on both F atoms toward the empty p (p^+) orbital on C_1 (n_F-p^+ charge transfer interactions)⁹ and the TS is stabilized as much as possible by preventing the formation of antiaromatic cyclopentadienyl cationic ring structure. The n_F-p^+ charge transfer energy ($\Sigma\Delta E^{(2)}_{n-p^+} = -295$ kcal mol⁻¹) is the main component of the total increase ($\Sigma\Delta E^{(2)}_{\sigma-\sigma^*} = -370$ kcal mol⁻¹ in Table 4) in the proximate charge transfer delocalization energies^{6,10} on going from the reactants to the TS. The TS is further stabilized by an extra, but partial, C-X bond formation (BE = 102 (X = F), 76 (Cl) and 65 (Br) kcal mol⁻¹).¹¹ Due to the substantially larger gain in the bond energy with X = F (ca. 54% bond cleavage and 46% bond formation) than with X = Cl and Br (ca. 60% bond cleavage and 40% bond formation) despite the weaker charge transfer stabilization with X = F (Table 5), the barrier height to the σ -attack S_N2 reaction decreases in the order Cl

Table 4. Electrostatic (ΔE_{es}), Deformation (ΔE_{def}) and Charge-Transfer ($\Sigma\Delta E_{\sigma-\sigma^*}^{(2)}$) Energies for the Halide Exchange reactions of Cyclopentadienyl Halides at the MP2/6-311+G** Level (in kcal mol⁻¹)

X	Paths	ΔE_{es}	ΔE_{def}	$-\delta\Sigma\Delta E_{\sigma-\sigma^*}^{(2)}$
F	S_N2	8	42	-370
	(s- S_N2) ^a	(-12)	(42)	(-131)
	β - S_N2' -syn	42	32	-235
	β - S_N2' -anti (TS)	24	8	-218
	β - S_N2' -anti (Int)	33	28	-238
	γ - S_N2' -syn	48	29	-148
	γ - S_N2' -anti	44	29	-145
Cl	S_N2	23	37	-383
	(s- S_N2) ^a	(-8)	(42)	(-111)
	β - S_N2' -syn	31	34	-237
	β - S_N2' -anti	40	25	-294
	γ - S_N2' -syn	38	30	-345
	γ - S_N2' -anti	30	31	-347
Br	S_N2	30	31	-379
	(s- S_N2) ^a	(-6)	(42)	(-106)
	β - S_N2' -syn	36	32	-278
	β - S_N2' -anti	21	27	-438
	γ - S_N2' -syn	38	27	-444
	γ - S_N2' -anti	28	28	-454

^aBackside attack for the saturated reactants (*i.e.*, cyclopentyl halides).
^b $\delta\Delta E_{\text{es}} = \Delta E_{\text{es}}(\text{TS}) - \Delta E_{\text{es}}(\text{Reactant})$. ^c $\delta\Sigma\Delta E_{\sigma-\sigma^*}^{(2)} = \Sigma\Delta E_{\sigma-\sigma^*}^{(2)}(\text{TS}) - \Sigma\Delta E_{\sigma-\sigma^*}^{(2)}(\text{Reactant})$.

($\Delta G^\ddagger = 10.1$ kcal mol⁻¹) > Br (8.9) > F (8.5), which is similar to the order of the S_N2 reactions with **2**, Cl ($\Delta G^\ddagger = 11.7$ kcal mol⁻¹) \cong Br (11.7) > F (7.0).

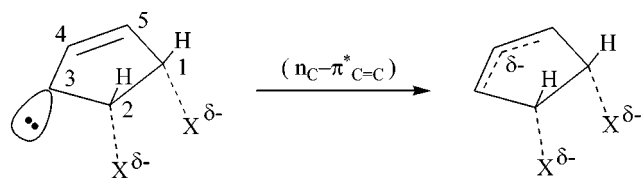
Comparisons of activation energies, $\delta\Delta G^\ddagger = \Delta G^\ddagger(S_N2) - \Delta G^\ddagger(s-S_N2)$, between those for the reactions of cyclopentadienyl halides (S_N2) with those corresponding reactions of the saturated, cyclopentyl, halides (s- S_N2), show that the reactivities of **1** with X = Cl ($\delta\Delta G^\ddagger = -1.6$ kcal mol⁻¹) and Br ($\delta\Delta G^\ddagger = -2.8$ kcal mol⁻¹) are faster by $k(S_N2)/k(s-S_N2) \cong 10$ and 10^2 at 298 K respectively, but is slower ($\delta\Delta G^\ddagger = +1.5$ kcal mol⁻¹) by 10^{-1} with X = F. The G2(+)/MP2 reactivity ratio of 10^2 is in good agreement with the experimental reactivity ratio, $k(S_N2)/k(s-S_N2) \cong 10^2$ for X = Br,¹ considering the fact that our theoretical values are for the gas-phase reactions whereas the experimental data are for the reactions of cyclopentadienyl (S_N2) and cyclopentyl (s- S_N2) bromides with $\Gamma(\text{Bu}_4\text{N}^+\Gamma^-)$ in $\text{CCl}_4\text{-CH}_3\text{CN}$ mixtures at 298 K.¹ The lower reactivity of cyclopentadienyl fluoride ($k(S_N2)/k(s-S_N2) \cong 10^{-1}$) than cyclopentyl fluoride is most probably due to the weak antiaromatic cyclopentadienyl cationic character of the TS with X = F, while the higher reactivity of cyclopentadienyl chloride and bromide than the corresponding cyclopentyl halides are due to the aromatic cyclopentadienyl anionic character of the TSs involved, as discussed above.

In general there are several factors that are important for the TS stability, and hence for the reactivity, in the S_N2 reactions: (i) The deformation energy, ΔE_{def} , that is needed to supply for the structural deformation of the reactant to achieve the TS structure. The major component of ΔE_{def} is

the stretching of the leaving group in the TS.¹² (ii) The bond energy (BE) gain in the newly formed ((partial) bond by the nucleophile. (iii) Changes in the proximate charge transfer energies (eq. 2) upon TS formation, $\delta\Delta E_{\sigma-\sigma^*}^{(2)} = \Delta E_{\sigma-\sigma^*}^{(2)}(\text{TS}) - \Delta E_{\sigma-\sigma^*}^{(2)}(\text{Reactants})$. The charge transfer interaction takes place between vicinal (and / or geminal) bond (n , π , σ , etc) and vacant antibond (π^* , σ^* , etc) orbitals, and the interaction energy can be calculated as the second-order perturbation energy by eq. 2.^{6,9} (iv) Changes in non-charge-transfer energies,⁶ $\delta\Delta E_{\text{NCT}} = \Delta E_{\text{NCT}}(\text{TS}) - \Delta E_{\text{NCT}}(\text{Reactants})$, upon TS formation. Non-charge-transfer term (ΔE_{NCT}) includes electrostatic (ΔE_{es}) and steric interaction energies (ΔE_{st}) and corresponds essentially to the energy associated with the Lewis structure (ΔE_{Lew}).¹³

The σ -attack S_N2 reactions of cyclopentadienyl halides (**1**) have relatively tight associative S_N2 type TS structures in which the bond formation (40-45%) and cleavage (54-60%) have progressed approximately 50% with negative charge development at the reaction center carbon (except with X = F). The major stabilization energy is provided by the $n_{\text{X}}-p^+$ interaction (-295 (F); -309 (Cl); -299 kcal mol⁻¹ (Br)). In addition to this charge delocalization toward the developing empty p (p^+) orbital at C₁, small but significant $\pi_{\text{C=C}}-p^+$ charge transfer (-50 (F); -68 (Cl); -74 kcal mol⁻¹ (Br)) occurs and the cyclopentadienyl ring acquires delocalized anionic (aromatic) character. For X = F, these charge delocalizations are not sufficient to gain aromatic character but is supplemented by the strong bond energy of a newly, but partially, formed C-F bond to stabilize the TS. Due to the slightly cationic antiaromatic character with X = F, the reaction barrier becomes higher than that for the saturated, cyclopentyl fluoride, in which there is no delocalization within the (saturated) ring. This means that other factors ((i) and (iv) above) differ very little and contribute similarly to the TSs for the reactions of **1** and **2**. Quite interestingly, the stabilizing factors in the TSs for **1** form a striking contrast to those in the TSs for cyclopropenyl halides (**5**). For the halide exchanges in **5**, the TSs are of the dissociative S_N2 type and have an "open" (loose) structure with low degree of bond making (22-33%) and extensive bond cleavage (67-78%).⁸ The cyclopropenyl ring becomes strongly positive (+0.67 ~ +0.76) and achieves strong aromatic cyclopropenyl cation structure. The major charge delocalization comes from the $\pi_{\text{C=C}}-p^+$ interaction (-307 ~ -367 kcal mol⁻¹) with small stabilizing electrostatic (-61 ~ -86 kcal mol⁻¹) and destabilizing deformation (35-46 kcal mol⁻¹) energies. Here due to the extensive stretching of the C-X bonds (very small overlap between the two orbitals leads to negligible Fock matrix element F_{p-p^+}) there is no $n_{\text{X}}-p^+$ type charge transfer interaction.

The π -attack β - S_N2' reactions. The nucleophile can attack at a neighboring β -carbon either with syn (β - S_N2' -syn) or anti (β - S_N2' -anti) orientation to the existing C-X bond forming a 1,2-dihalocyclopentenyl anion like TS. The anti 1,2-dihalo adduct is stable enough to exist as an intermediate only for X = F with a well-depth of -3.5 kcal mol⁻¹ at the G2(+)/MP2 level, and the β - S_N2' -anti reaction with X = F

Scheme 2. β - $S_{N2'}$ -syn TS.

exhibits a triple-well potential energy profile. The stable 1,2-dihalo adducts are not formed with $X = \text{Cl}$ and Br , so that β - $S_{N2'}$ reactions with $X = \text{Cl}$ and Br proceed by a double-well potential energy surfaces. The energetics in Tables 1-3 reveals that the B3LYP activation energies are lower than those corresponding values at the G2(+)/MP2 level, excepting for the two cases of β - $S_{N2'}$ -syn TS and β - $S_{N2'}$ -anti adduct with $X = \text{F}$ for which the reverse holds, *i.e.*, the B3LYP ΔG^\ddagger values are higher. This suggests that the DFT method overestimates electron correlation effects in general for the delocalized TS,^{14,15} but underestimates interorbital pair correlation energies between neighboring lone pairs on the two F atoms¹⁶ of the vicinal C-F bonds which are much shorter ($d_{\text{C-F}}^\ddagger = 1.438 \text{ \AA}$) than those of C-Cl (1.879 \AA) and C-Br (2.129 \AA) in the β - $S_{N2'}$ -syn TS. The β - $S_{N2'}$ TSs are relatively tight (**S2**) with large degree of bond formation (75-93%) and small extent of bond cleavage (7-25%) in the syn TSs compared with the corresponding values of 53-71% and 6-47% in the anti TSs.

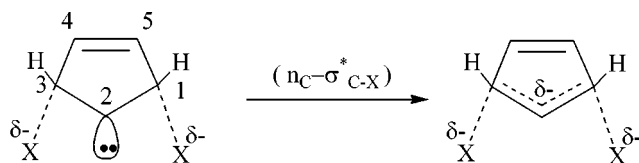
On the other hand, the MP2 ΔG^\ddagger values for the β - $S_{N2'}$ paths with $X = \text{Cl}$ and Br are lower than those corresponding values at the G2(+)/MP2 level. This indicates that, in contrast to underestimation of electron correlation effects in general at the MP2 level, they are overestimated for the delocalized TSs^{14,15} of the β - $S_{N2'}$ paths with $X = \text{Cl}$ and Br . The NBO analyses indicate that in both the syn and anti TSs of the β - $S_{N2'}$ paths, an incipient lone pair formed on C_3 is delocalized toward the $\text{C}=\text{C}$ bond by a strong $n_{\text{C}}-\pi_{\text{C}=\text{C}}^*$ charge transfer interaction and the delocalized allyl anionic structure is formed over C_3 - C_4 - C_5 moiety as shown in Scheme 2. The lone pair on C_3 is a p type in the anti path, whereas it is an sp^3 type in the syn path. This $n_{\text{C}}-\pi_{\text{C}=\text{C}}^*$ charge transfer delocalization provides major part (> 80%) of the overall proximate charge transfer energies listed in Table 4. There are also weak vicinal $n_{\text{C}}-\sigma_{\text{C-X}}^*$ interactions in all of the β - $S_{N2'}$ TSs. This means that electronic delocalization extends partly to C_2 , *i.e.*, over C_2 - C_5 moiety (Scheme 2). The overall proximate charge transfer energies ($-\delta\Delta E_{\sigma-\sigma}^{(2)*}$) summarized in Table 4 show that the anti TSs (compare the adduct value for the anti path with $X = \text{F}$) have stronger stabilization than the syn TSs due to the proximate charge transfer delocalization leading to lower activation energies for the anti β - $S_{N2'}$ reactions. The β - $S_{N2'}$ -syn TSs (C_s symmetry) for $X = \text{Cl}$ and Br are characterized by two imaginary frequencies at the MP2/6-311+G** level indicating that they are second-order saddle points with a maximum with respect to two mutually perpendicular directions.¹⁷ Such a TS may be considered as a transient structure in the inversion profile of the β - $S_{N2'}$ -anti TSs (C_2 symmetry) and has an energy

higher by 13-20 kcal mol⁻¹ at the G2(+)/MP2 level than the C_2 structure. The higher ΔG^\ddagger values for the syn than anti path are in most cases due to higher steric repulsion ($\Delta E_{\text{es}} > 0$) as evident from more negative ΔS^\ddagger value by *ca.* 2-4 e.u. for the syn path, and also due to higher deformation energies (ΔE_{def}) for the syn (Table 4) than the anti path.

For the β - $S_{N2'}$ reaction paths also the fluoride exchanges have considerably lower activation energies despite low proximate charge transfer stabilizations, *e.g.*, for the anti path, $\Delta G^\ddagger = -1.0$ (F), 20.2 (Cl) and 18.6 kcal mol⁻¹ (Br). Since stretching of the C-F bond in the TS is smaller than that of the C-Cl and C-Br bond the ΔE_{def} value is smaller for $X = \text{F}$ by *ca.* 17-19 kcal mol⁻¹ than for $X = \text{Cl}$ and Br . We also invoke the bond energy factor (factor (ii), *vide supra*) to rationalize the considerably lower ΔG^\ddagger value with $X = \text{F}$ since bond energy of the C-F bond is much stronger than those of the C-Cl and C-Br bonds.¹¹ This interpretation was also applicable to the lower ΔG^\ddagger values with $X = \text{F}$ for the halide exchanges in cyclopropenyl halides.⁸

The activation energies (ΔG^\ddagger) for the β - $S_{N2'}$ processes of halide exchanges in cyclopropenyl halides, (**5**), are substantially lower than the corresponding reactions with **1**, especially with $X = \text{Cl}$ [lower by *ca.* 20 ((syn) and 14 kcal mol⁻¹ (anti))] and with Br [by *ca.* 25 (syn) and 15 kcal mol⁻¹ (anti)]. A possible origin of this activation energy differences could be the more delocalized (covering whole cyclopropene ring) 1,2-dihalocyclopropyl anion-like TSs than the partially delocalized (covering only three carbon atoms out of five of the ring) 1,2-dihalocyclopentenyl anion-like TSs. In both cases, there is no involvement of aromatic vs antiaromatic character of small rings, since in the former the TS is cyclopropyl (not cyclopropenyl) anion like, whereas in the latter the TS has cyclopentenyl (not cyclopentadienyl) anion like structure.

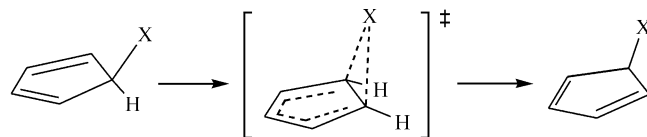
The π -attack γ - $S_{N2'}$ reactions. The nucleophile can substitute at a γ -carbon with a double well potential energy surface leading either to a syn (γ - $S_{N2'}$ -syn) or anti (γ - $S_{N2'}$ -anti) orientation to the C-X bond in the TS. No stable γ -adduct was found at all levels of theory. Reference to Tables 1-3 reveals that the B3LYP ΔG^\ddagger (ΔE^\ddagger) values for the γ - $S_{N2'}$ -syn paths with $X = \text{Cl}$ and Br are higher than those for the γ - $S_{N2'}$ -anti paths in contrast to the lower G2(+)/MP2 ΔG^\ddagger values (except for $X = \text{Br}$, $\Delta G^\ddagger(\text{syn}) \cong \Delta G^\ddagger(\text{anti})$) indicating that the interorbital pair electron correlation effects between the lone pairs on the two halogen atoms of the eclipsing C-X bonds (and also lone pairs on C_2) in the γ - $S_{N2'}$ -syn TSs are underestimated as in the β - $S_{N2'}$ -syn paths (*vide supra*). The MP2 ΔG^\ddagger values (Table 2) are all higher than those at the G2(+)/MP2 level (Table 3) so that electron correlation effects for the γ - $S_{N2'}$ TSs are underestimated at the MP2 level. This is in contrast to the overestimation of electron correlation effects at the MP2 level for the β - $S_{N2'}$ TSs due to strong electronic charge delocalized structures.^{14,15} This means that the electronic charge delocalization in the γ - $S_{N2'}$ TSs is weaker than that in the β - $S_{N2'}$ TSs in which delocalization occurs partially over four carbon atoms, C_2 - C_5 (Scheme 2), as discussed above. The TS structures are shown in Figures

Scheme 3. γ -S_N2'-syn TS.

1-3. A lone pair develops at the β -(C₂) position in the γ -S_N2' TSs, scheme 3, a p type for the anti and an sp^3 type for the syn, and relatively strong $n_C-\sigma^*_{C-X}$ vicinal charge transfer interactions occur and the C₁-C₂-C₃ moiety becomes a delocalized allyl anion. There are also very weak $\pi_{C=C}-\sigma^*_{C-X}$ charge transfer interactions; the $\Delta E_{p-s}^{(2)*}$ values range -8 (X = F) ~ -16 (X = Br) kcal mol⁻¹ whereas the $\Delta E_{n-\sigma}^{(2)*}$ values are much greater than these ranging -67 (X = F) ~ -219 (X = Br) kcal mol⁻¹. These latter $\Delta E_{n-\sigma}^{(2)*}$ charge transfer energies in the γ -S_N2' TSs are, however, considerably lower than the $n_C-\pi^*_{C=C}$ interaction energies ($\Delta E_{n-\pi}^{(2)*} = -198 \sim -334$ kcal mol⁻¹) in the β -S_N2' TSs (Scheme 1) mainly due to wider energy gaps, ($\Delta\epsilon = \epsilon_{\sigma^*} - \epsilon_n$ in eq. 2) with the lower n levels [*e.g.*, $\epsilon_n = 0.022$ (syn) and 0.019 a.u. (anti) in the γ -S_N2' TS vs $\epsilon_n = 0.025$ (syn) and 0.026 a.u. (anti) in the β -S_N2' TSs for X = Cl] and the higher σ^*_{C-F} than $\pi^*_{C=C}$ levels. The γ -S_N2' TSs are somewhat looser with lower degree of bond formation and larger degree of bond cleavage than the β -S_N2' TSs. For example all the C-X bonds for the γ -S_N2' in Figures 1-3 are longer than those for the β -S_N2' TSs. The negative charges on C₂ in the γ -S_N2' TSs are stronger (*e.g.*, for X = Cl $q_2 = -0.402$ (syn) and -0.397 (anti)) than those on C₄ in the β -S_N2' TSs (*e.g.*, for X = Cl, $q_4 = -0.186$ (syn) and -0.161 (anti)). This means that the lone pairs on C₂ in the γ -S_N2' TSs are less delocalized (or more localized) than those on C₄ in the β -S_N2' TSs.

The proximate charge transfer stabilization ($-\delta\Sigma\Delta E_{\sigma-\sigma}^{(2)*}$ in Table 4) of the γ -S_N2' TS increases in the order X = F < Cl < Br. However, the barrier height decreases in the order Cl ($\Delta G^\ddagger \cong 19$ kcal mol⁻¹) > Br (17) > F (3-5); in other words the halide exchanges of fluoride have the lowest proximate charge transfer TS stabilization but have the highest reactivity. These trends of the lowest charge transfer delocalization with the highest reactivity for X = F in the γ -S_N2' processes are similar to those found in the β -S_N2' processes. We interpret this highest reactivity with X = F as the stronger gain of the C-F bond energy relative to C-Cl and C-Br bonds in the β - as well as γ -S_N2' TSs.

Although the differences in the ΔG^\ddagger values between γ -S_N2'-syn and anti processes are almost insignificant for X = Cl and Br, there is *ca.* 2 kcal mol⁻¹ difference in favor of the γ -S_N2'-syn for X = F. This appears to be caused by the

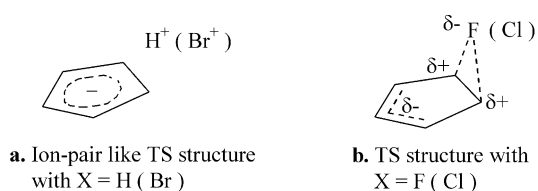


Scheme 4. 1,5-Sigmatropic rearrangements.

Table 5. Energetics^a for Circumambulatory Rearrangements of Cyclopentadienyl Halides, Calculated at Various Methods with 6-311+G** Basis Sets (in kcal mol⁻¹)

Method	X	ΔE^\ddagger	ΔE^\ddagger_{ZPE}	ΔH^\ddagger^b	$-\Delta TS^\ddagger^b$	ΔG^\ddagger^b
B3LYP	H	27.52	25.47	25.26	-0.06	25.20
	F	44.87	43.43	43.34	0.25	43.59
	Cl	27.83	26.88	26.70	0.39	27.10
	Br	21.91	21.11	20.87	0.49	21.36
MP2	H	25.32	23.19	22.99	-0.06	22.93
	F	52.84	51.66	51.51	0.37	51.88
	Cl	34.37	33.79	33.52	0.61	34.14
	Br	26.93	26.36	26.08	0.65	26.72
G2(+)-MP2 ^c	H	28.58	26.45	26.25	-0.06	26.19
	F	50.85	49.67	49.52	0.37	49.89
	Cl	33.60	33.03	32.76	0.61	33.37
	Br	26.95	26.38	26.09	0.65	26.74

^aCorrected for zero-point vibrational energy with appropriate scaling factors: 0.9806 for the B3LYP method, and 0.9748 for the MP2 method. ^bAt 298 K. ^cThe MP2 geometries were used, and thermal data were taken from the MP2/6-311+G** level.



Scheme 5

stronger $n_C-\sigma^*_{C-F}$ interaction in the syn (-68.8 kcal mol⁻¹) than anti (-66.7 kcal mol⁻¹) leading to stronger delocalized allyl anionic moiety (C₁-C₂-C₃) as evidenced by the lower negative charge on C₂ for syn (-0.609) than anti (-0.619). In fact the lower activation energy for the syn than anti paths by 2 kcal mol⁻¹ is the same as the difference in the $n_C-\sigma^*_{C-F}$ charge transfer energy difference.

Circumambulatory rearrangements. The halogen atom in the cyclopentadienyl halides can undergo sigmatropic rearrangement by 1,5-shift and migrates around the periphery of the five-membered conjugated ring in a so-called monohapto (1,5-suprafacial) circumambulatory (merry-go-round) rearrangement reaction,³ Scheme 4. We have used four migrants (X = H, F, Cl and Br) and the activation energies calculated at the B3LYP, MP2 and G2(+)-MP2 levels are summarized in Table 5. The ΔG^\ddagger values at the B3LYP level are lower than those corresponding values at the G2(+)-MP2 level, due to the overestimation of electron correlation effects in the TSs. The barrier heights increase in the order X = H < Br < Cl < F at the MP2 and G2(+)-MP2 levels, but the barrier height for X = H rises higher than that for X = Br at B3LYP level. Moreover, the ΔG^\ddagger value for X = H (and Br) at the MP2 level is lower than that at the G2(+)-MP2 level. The origin of this lower ΔG^\ddagger values at the MP2 than G2(+)-MP2 level for X = H is again the overestimation of electron correlation effects for the relatively strong charge delocalized TS structure^{14,15} with X = H at the MP2 level. The percentage bond order changes, $\% \Delta n^\ddagger$ (S4), reveal that

the TS with X = H has a particularly tighter structure (65% bond formation; 35% bond cleavage) than those with other migrants (for X = F, Cl and Br, bond formation is *ca.* 40% and bond cleavage is *ca.* 60%). The NPA charges (**S5**) at the NBO-MP2/6-311+G** level show that negative charge delocalization over the ring is the strongest with X = H ($q_1 = q_2 = -0.340$, $q_3 = q_5 = -0.252$ and $q_4 = -0.236$) and the weakest with X = F ($q_1 = q_2 = +0.035$, $q_3 = q_5 = -0.365$ and $q_4 = -0.024$). Furthermore, the formal charge of the migrant in the TS (**S5**) is positive with X = H ($q_X = +0.341$) and X = Br ($q_X = +0.033$), while it is negative for X = F and Cl. These NPA charge analyses (**S5**) indicate that the TS structure with X = H (and to a smaller extent with X = Br) is nearly an ion pair type, (Scheme 5a) with charge delocalized cyclopentadienyl anionic (aromatic) ring. On the other hand, the TS with X = F (and to a lesser degree with X = Cl) has a quadrupole structure (Scheme 5b) with little charge delocalization within the ring. The ion pair like TS with X = H (and with Br) is stabilized by an aromatic cyclopentadienyl anion like ring structure. This is in sharp contrast to the strong antiaromatic negative charge delocalized ring structure found in the sigmatropic 1,3-shift for cyclopropene (X = H) with extremely high activation energy, $\Delta G^\ddagger = 88.5 \text{ kcal mol}^{-1}$ at the G2(+)-MP2 level.⁸ These trends of extremely high energy barrier to the 1,3-sigmatropic hydride shift on the cyclopropene ring in contrast to much lower barrier to the 1,5-sigmatropic hydride shift on the cyclopentadiene ring ($\Delta G^\ddagger = 26.2 \text{ kcal mol}^{-1}$ at the G2(+)-MP2 level) are consistent with the experimental results; thermally induced 1,3-hydride shifts have not been reported for simply substituted cyclopropenes,^{3,18} whereas the corresponding 1,5-sigmatropic hydride shifts for cyclopentadiene are known to be facile at *ca.* 60 °C with a barrier height of $\Delta G^\ddagger = 24.3 \text{ kcal mol}^{-1}$.¹⁹ In fact circumambulation around cyclopentadiene ring is not limited to hydride as the migrating group.³ A wide variety of other types of groups can undergo comparable thermally induced migration. Alkyl groups shift in general with substantially higher activation energies (*e.g.*, methyl group shifts at *ca.* 200 °C with $\Delta G^\ddagger = 41.8 \text{ kcal mol}^{-1}$)²⁰ than hydride.

We have correlated the activation energy (ΔG^\ddagger at the G2(+)-MP2 level) for the circumambulatory rearrangement of X

$$\Delta G^\ddagger = (0.29 \pm 0.03)\text{BE} + (11.79 \pm 0.59)\chi - (26.54 \pm 2.40) \quad (4)$$

$(r = 0.999)$

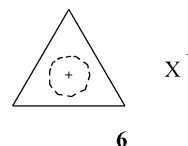
(= H, F, Cl and Br) with bond energy (BE) of the C-X bond and electronegativity (χ) of X, eq. 4. For the cyclopentadienyl ring, both the BE and electronegativity (χ)²¹ contribute to elevate the barrier height,⁴ *i.e.*, the stronger the BE and the electronegativity, the barrier becomes higher. Alternatively, a migrant X with low electronegativity and weak C-X bond will readily form a $((\text{C}_5\text{H}_5)^- + \text{X}^+)$ like TS (Scheme 5), which is stabilized by an aromatic cyclopentadienyl anion ring. By contrast, the same type of correlation with ΔG^\ddagger (G2(+)-MP2) values⁸ for circumambulatory rearrangement of X (= H, F, Cl and Br) in the cyclopropenyl

ring, eq. 5, leads to a negative coefficient of χ . This means

$$\Delta G^\ddagger = (1.34 \pm 0.09)\text{BE} - (41.38 \pm 2.36)\chi + (36.16 \pm 8.76) \quad (5)$$

$(r = 0.997)$

that an aromatic cyclopropenyl cation- X^- ion pair like⁵ TS, (**6**), formation is facilitated by a strong electronegativity of X.



We therefore conclude that the lower activation energies with X = H and Br than with X = F and Cl are due to strong (delocalized) negative charge development in the ring (as evidenced by the overestimation of electron correlation effects at the MP2 level) in the TS leading to aromatic cyclopentadienyl anion ring structure.

Relative reactivities. For the gas-phase identity nucleophilic reaction pathways of fluoride anion with cyclopentadienyl fluoride, the *reactivity* increases at the G2(+)-MP2 level in the order $\text{S}_\text{N}2 < \gamma\text{-S}_\text{N}2'\text{-anti} < \gamma\text{-S}_\text{N}2'\text{-syn} < \beta\text{-S}_\text{N}2'\text{-syn} < \beta\text{-S}_\text{N}2'\text{-anti}$. The lowest reactivity of $\text{S}_\text{N}2$ path with X = F is due to the weak antiaromatic cationic ring structure in the TS while the highest reactivity with $\beta\text{-S}_\text{N}2'\text{-anti}$ can be attributed to the formation of a stable 1,2-difluorocyclopentenyl anion, which in turn is stabilized by the strong $\text{n}_\text{C}-\pi^*_{\text{C}=\text{C}}$ charge transfer interaction with a delocalized allylic anion structure. The strong C-F bond energy in the adduct also contributes to its stability. The sigmatropic 1,5-shift of F has much higher activation barrier with $49.9 \text{ kcal mol}^{-1}$ than other fluoride exchange reaction paths so that can not interfere or compete with other reaction path.

For the reactions with X = Cl, the σ -attack $\text{S}_\text{N}2$ reaction path is the most favored and has the strongest reactivity; the reactivity increases in the order at the G2(+)-MP2 level, $\beta\text{-S}_\text{N}2'\text{-syn} < \beta\text{-S}_\text{N}2'\text{-anti} < \gamma\text{-S}_\text{N}2'\text{-syn} < \gamma\text{-S}_\text{N}2'\text{-anti} < \text{S}_\text{N}2$. The strongest reactivity of the σ -attack $\text{S}_\text{N}2$ path is ascribed to the weak aromatic cyclopentadienyl anion like TS. For X = Cl, the two $\gamma\text{-S}_\text{N}2'$ paths, *i.e.*, syn and anti, have similar reaction barriers, *ca.* 19 kcal mol^{-1} , which are lower than those for the $\beta\text{-S}_\text{N}2'$ paths. The high energy barrier with $\beta\text{-S}_\text{N}2'\text{-syn}$ is due to smaller proximate charge transfer stabilization (Table 4). The sigmatropic 1,5-shift of chlorine atom has also a high energy barrier, $33.4 \text{ kcal mol}^{-1}$ at the G2(+)-MP2 level, which is considerably higher than those for all halide exchange reaction paths except for the $\beta\text{-S}_\text{N}2'\text{-syn}$ path which has almost the same barrier height of $33.6 \text{ kcal mol}^{-1}$. Thus the circumambulatory rearrangement reaction of chlorine can not compete with halide exchange reactions in general, in particular with the σ -attack $\text{S}_\text{N}2$ path ($\Delta G^\ddagger = 10.1 \text{ kcal mol}^{-1}$) which is favorable by more than 20 kcal mol^{-1} over the sigmatropic 1,5-shift.

For the reactions of X = Br, the reactivity trends are similar to those of X = Cl above: the σ -attack $\text{S}_\text{N}2$ path is the

most favored due to the aromatic cyclopentadienyl anion like TS structure. Again the two γ - S_N2' paths have similar energy barriers, *ca.* 17 kcal mol⁻¹. The β - S_N2' -syn path has the highest energy barrier (36.6 kcal mol⁻¹), which is even higher than the sigmatropic 1,5-shift of the bromine atom (26.7 kcal mol⁻¹). The much higher barrier for β - S_N2' -syn (by 20 kcal mol⁻¹) than for β - S_N2' -anti results from much lower proximate charge transfer energies [-278 (syn) *vs* -438 (anti) kcal mol⁻¹, Table 4]. For β - S_N2' bromide exchanges, the energy gaps between n_C and σ_{C-Br}^* levels are 0.30 (syn) and 0.21 a.u. (anti) so that the n_C - σ_{C-Br}^* charge delocalization energies are -57 (syn) *vs* -178 (anti) kcal mol⁻¹, and lead to large overall proximate charge transfer energy difference cited above. The activation barrier to the circumambulatory bromine migration is low with 26.7 kcal mol⁻¹, but is still higher than all the halide exchange paths except for β - S_N2' -syn path. Therefore the Br migration can not compete with the halide exchanges, especially with the σ -attack S_N2 path. The reactivity increases in the order 1,5-shift < β - S_N2' -syn < β - S_N2' -anti < γ - S_N2' -syn \cong γ - S_N2' -anti < S_N2 .

For the reactions with X = F, the β - S_N2' paths are the most preferred and the σ -attack S_N2 path is the most disfavored. In contrast, however, for the reactions with X = Cl and Br, the most preferred path is the σ -attack S_N2 and the S_N2' paths are much less favored (by more than 8 kcal mol⁻¹) relative to the S_N2 process. We therefore conclude that in the gas phase the chloride and bromide exchanges in the corresponding cyclopentadienyl halides (**1**) proceed by the σ -attack S_N2 path and the S_N2' processes should be difficult to compete and will constitute the minor reaction pathways. This conclusion supports the experimentally deduced S_N2 mechanism of Breslow *et al.* for the halide exchanges in cyclopentadienyl halides.¹ However, the possibility of competing the γ - S_N2' path (as well as the β - S_N2' path) with the S_N2 reaction raised by them can be disregarded.¹ Our results also show that reactions involving displacement on the halogen atom to form a dihalogen molecule leading to cyclopentadienyl anion formation is not possible in the gas phase.¹

The gas phase fluoride exchange reaction exhibits entirely different trends compared to chloride and bromide exchanges. The TSs in the fluoride exchanges are mostly stabilized by an extra, albeit partial, strong C-F bond energy, which seems to provide much lower energy barriers to β - as well as γ - S_N2' reactions but not in the S_N2 path since F is bound much looser ($d_{C-F}^\ddagger = 1.856$ Å *vs* $d_{C-F}^\ddagger = 1.438$ and 1.541 Å in the β - and γ - S_N2' TSs respectively).

The barrier heights at the G2(+)-MP2 level increase in the order X = F < Br < Cl for all the gas-phase identity halide exchanges in the cyclopentadienyl halides. This order is the same as that found for the gas-phase identity methyl transfer reactions²² and also for the π -attack S_N2' paths of the halide exchange reactions of cyclopropenyl halides (**5**) at the G2(+) level of theory.⁸ In the latter reactions of **5**, the barrier heights of the σ -attack S_N2 paths are strongly dependent on the development of positive charge in the cyclopropenyl ring, an aromatic cyclopropenium ion character, in the TS,

which decreases in the order X = Br > Cl > F so that the barrier heights increase in the order X = Br < Cl < F. The lowest degree of positive charge development with X = F in this case is the results of rather tighter TS with larger degree of bond formation and lower degree of bond cleavage than those with X = Cl and Br. Thus there is a compromise between a greater degree of aromatic ring formation (the looser the better) and the stronger bond energy gain (the tighter the better) for the S_N2 TS with X = F.

Finally it is appropriate here to summarize the relationship between electron correlation effects calculated and delocalization within a TS or an intermediate. (i) Electron correlation enhances delocalization. Various resonance delocalized forms of a molecular species are already present at the uncorrelated MO level, but electron correlation provides larger weights to the resonance delocalized forms rather than new types of resonance delocalization. This is why the activation barriers to reactions with a delocalized TS become lower with correlated than uncorrelated MOs. Ample examples are presented by Weinhold and coworkers.^{6b,c} (ii) The electron correlation effects are in general underestimated at the MP2 level, but for electron delocalized structures the electron correlation effects are overestimated.^{14,15} We encounter often a reaction with delocalized TS, for which the electron correlation effects are overestimated and hence the activation energy is underestimated at the MP2 level relative to a higher level (*e.g.*, G2 level) result. Examples: The lower β - S_N2' reaction barriers with X = Cl and Br at the MP2 level (Table 2) than the corresponding values at the G2(+)-MP2 level (Table 3). (iii) The electron correlation effects are overestimated in the DFT (*e.g.*, B3LYP) energetics especially for a delocalized structure so that for reactions with a delocalized TS the activation energies are underestimated.¹⁵ However, the interorbital pair correlation energies between lone pairs on neighboring atoms are underestimated, and hence if such neighboring lone-pairs are present in the TS, the activation energy is overestimated. Examples: The higher DFT ΔG^\ddagger (ΔE^\ddagger) values (Table 1) than the corresponding values at the G2(+)-MP2 level (Table 3) for β - S_N2' -syn (TS) and β - S_N2' -anti (intermediate) processes.

These trends of accounting for electron correlation effects at lower levels of theory can therefore help understanding TS structures as the examples given above demonstrate.

Acknowledgment. This work was supported by Korea Research Foundation Grant (KRF-2000-015-DP0208).

References

1. Breslow, R.; Canary, J. W. *J. Am. Chem. Soc.* **1991**, *113*, 3950.
2. (a) Minkin, V. I.; Glukhovtsev, M. N.; Simkin, B. Y. *Aromaticity and Antiaromaticity*; Wiley: New York, 1994. (b) Breslow, R. *Acc. Chem. Res.* **1973**, *6*, 395. (c) Reindl, B.; Schleyer, P. v. R. *J. Comput. Chem.* **1998**, *19*, 1402. (d) Glukhovtsev, M. N.; Bach, R. D.; Laiter, S. *J. Phys. Chem.* **1996**, *100*, 10952. (e) Lee, E. P. F.; Wright, T. G. *Phys. Chem. Chem. Phys.* **1999**, *1*, 219.
3. Childs, R. F. *Tetrahedron* **1982**, *38*, 567.
4. Frisch, M. J.; Trucks, G. W.; Schlegel, H. B.; Scuseria, G. E.;

- Robb, M. A.; Cheeseman, J. R.; Zakrzewski, V. G.; Montgomery, J. A. Jr.; Stratmann, R. E.; Burant, J. C.; Dapprich, S.; Millam, J. M.; Daniels, A. D.; Kudin, K. N.; Strain, M. C.; Farkas, O.; Tomasi, J.; Barone, V.; Cossi, M.; Cammi, R.; Mennucci, B.; Pomelli, C.; Adamo, C.; Clifford, S.; Ochterski, J.; Petersson, G. A.; Ayala, P. Y.; Cui, Q.; Morokuma, K.; Malick, D. K.; Rabuck, A. D.; Raghavachari, K.; Foresman, J. B.; Cioslowski, J.; Ortiz, J. V.; Stefanov, B. B.; Liu, G.; Liashenko, A.; Piskorz, P.; Komaromi, I.; Gomperts, R.; Martin, R. L.; Fox, D. J.; Keith, T.; Al-Laham, M. A.; Peng, C. Y.; Nanayakkara, A.; Gonzalez, C.; Challacombe, M.; Gill, P. M. W.; Johnson, B.; Chen, W.; Wong, M. W.; Andres, J. L.; Head-Gordon, M.; Replogle, E. S.; Pople, J. A. *Gaussian 98, Revision A.6*; Gaussian, Inc.: Pittsburgh, PA, 1998.
5. Scott, A. P.; Radom, L. *J. Phys. Chem.* **1996**, *100*, 16502.
6. (a) Reed, A. E.; Curtiss, L. A.; Weinhold, F. *Chem. Rev.* **1988**, *88*, 899. (b) Glendening, E. D.; Badenhop, J. K.; Weinhold, F. *J. Comput. Chem.* **1998**, *19*, 593. (c) Glendening, E. D.; Badenhop, J. K.; Weinhold, F. *J. Comput. Chem.* **1998**, *19*, 628.
7. (a) Houk, K. N.; Gustafson, S. M.; Black, K. *J. Am. Chem. Soc.* **1992**, *114*, 8565. (b) Lee, I.; Kim, C. K.; Lee, B.-S. *J. Comput. Chem.* **1995**, *16*, 1045. (c) Lee, J. K.; Kim, C. K.; Lee, I. *J. Phys. Chem. A* **1997**, *101*, 2893.
8. Kim, C. K.; Li, H. G.; Lee, B.-S.; Kim, C. K.; Lee, H. W.; Lee, I. *J. Org. Chem.* **2002**, *67*, 1953.
9. Epiotis, N. D.; Cherry, W. R.; Shaik, S.; Yates, R.; Bernardi, F. *Structural Theory of Organic Chemistry*; Springer-Verlag: Berlin, 1977; p 158.
10. Ref. 9, Part IV.
11. (a) The bond energies (BE) of the C-X bond in (CH)₅-X were calculated at the G2(+)/MP2//MP2/6-311+G** level in terms of enthalpies. (b) Klumpp, G. W. *Reactivity in Organic Chemistry*; Wiley: New York, 1982; p 38. BEs for C-X are given as 116 kcal mol⁻¹ (X = F), 81 (Cl) and 68 (Br).
12. Mitchell, D. J.; Schlegel, H. B.; Shaik, S. S.; Wolfe, S. *Can. J. Chem.* **1985**, *63*, 1642.
13. Carballeira, L.; Perez-Juste, I. *J. Phys. Chem. A* **2000**, *104*, 9362.
14. Raghavachari, K.; Whiteside, R. A.; Pople, J. A.; Schleyer, P. v. R. *J. Am. Chem. Soc.* **1981**, *103*, 5649.
15. Li, H. G.; Kim, C. K.; Lee, B.-S.; Kim, C. K.; Rhee, S. K.; Lee, I. *J. Am. Chem. Soc.* **2001**, *123*, 2326.
16. Similar underestimations of interorbital pair energies by B3LYP method involving neighboring lone pairs in F and Cl atoms have been reported. Petersson, G. A.; Malik, D. K.; Wilson, W. G.; Ochterski, J. W.; Montgomery, J. A. Jr.; Frisch, M. J. *J. Chem. Phys.* **1998**, *109*, 10570. See also Ochterski, J. W.; Petersson, G. A.; Montgomery, J. A. Jr. *J. Chem. Phys.* **1996**, *104*, 2598.
17. (a) Schlegel, H. B. In *Ab Initio Methods in Quantum Chemistry. Part I*; Lawley, K. P., Ed.; Wiley: Chichester, 1987; p 249. (b) Li, H. G.; Kim, C. K.; Lee, B.-S.; Kim, C. K.; Rhee, S. K.; Lee, I. *J. Am. Chem. Soc.* **2001**, *123*, 2326.
18. Sublett, B.; Bowman, N. S. *J. Org. Chem.* **1961**, *26*, 2594.
19. (a) Roth, W. *Tetrahedron Lett.* **1964**, 1009. (b) Bernardi, F.; Robb, M. A. In *Ab Initio Methods in Quantum Chemistry. Part I*; Lawley, K. P., Ed.; Wiley: Chichester, 1987; p 155.
20. McLean, S.; Findlay, D. M. *Can. J. Chem.* **1970**, *48*, 3107.
21. McWeeny, R. *Coulson's Valence*, 3rd ed.; Oxford Univ. Press: Oxford, 1979; p 163.
22. (a) Glukhovtsev, M. N.; Pross, A.; Radom, L. *J. Am. Chem. Soc.* **1995**, *117*, 2024. (b) Lee, I.; Kim, C. K.; Sohn, C. K.; Li, H. G.; Lee, H. W. *J. Phys. Chem. A* **2002**, *106*, 1081.